STAR-IRS Assisted Rate Splitting Multiple Access with Perfect and Imperfect CSI for 6G Communication

Aswini Krishnan, *Graduate Student Member, IEEE*, Sundaresan Sabapathy, *Graduate Student Member, IEEE,* and Surendar Maruthu, *Member, IEEE*

***Abstract*—Incorporating cutting-edge technology like rate splitting multiple access (RSMA) and intelligent reflecting surface (IRS) are essential in 6G communications to satisfy the constantly growing needs for more connection, better reliability, and faster data rates. This paper explores the concept of simultaneously transmitting and reflecting IRS (STAR-IRS) assisted RSMA in the presence of both perfect and imperfect channel state information (CSI). STAR-IRS leverages its dual capability to transmit and reflect signals simultaneously, enhancing spectral efficiency and expanding coverage. So far, in literature, STAR-IRS assisted RSMA system is analyzed in terms of outage probability with perfect CSI scenario. So, in this work, we carry out the performance analysis of STAR-IRS over imperfect CSI scenario in terms of outage probability and sum rate. Firstly, we derive the analytical expression of the outage probability and sum rate. Secondly, we propose a automatic optimization (AO) algorithm for weighted sum rate (WSR) maximization over imperfect CSI scenario. The performance analysis is carried out by varying power allocation factor to find its optimality. The derived outage probability and sum rate expressions are validated with Monte Carlo simulations. Also, it is found that AO-based algorithm enhances the weighted sum rate performance over imperfect CSI scenarios for STAR-IRS based RSMA systems.**

Link to graphical and video abstracts, and to code: https://latamt.ieeer9.org/index.php/transactions/article/view/9185

***Index Terms*—STAR-IRS, RSMA, outage probability, weighted sum rate, optimization, and channel estimation error.**

I. Introduction

PRESENTLY, reconfigurable intelligent surfaces (RISs), commonly called as intelligent reflecting surface (IRS), has gained attention which potentially enhances the network coverage and data rate in an effective way for global wireless connectivity in fifth generation and beyond (5GB) communication [1], [2]. Generally, an IRS is a planar array, based on metamaterials with affordable passive reflecting elements which can intelligently control the amplitude and phase shift of the reflected signal [3]. In short, an IRS dynamically adjusts the wireless environment to improve communication between base station and receivers in cases where direct connections have poor signal quality. IRSs are widely installed on building faces, walls, and ceilings to improve communication [4]. The principle of IRS is comparable to massive multiple-input multiple-output (MIMO) technology, which uses many antennas to increase spectrum and energy efficiency. As a result, IRS can play an important role in 6G communication networks. Also, IRS provides a possible path for facilitating the implementation of massive MIMO 2.0 [5]. IRS are intended only to reflect the incident signal in a desired direction. However, it cannot serve the users behind the IRS which is reported as a limitation in [6], [7]. Alternatively, IRSs that transmit and reflect simultaneously (STAR-IRSs), have emerged as a potential technology in which the IRSs allow incident wireless signals to either be reflected inside the half-space at the reflection side, or they can be transmitted (refracted) into one side of the IRS [8]. The STAR elements provide excellent coverage for all users in a 360° ground plane and adaptable wireless settings compared to conventional IRS elements [9]. In [10], the complexities of the STAR-IRS assisted MIMO network was investigated, using the novel energy splitting (ES) approach to improve the weighted sum rate. This technique showed considerable improvements, notably in non-orthogonal multiple access (NOMA) systems running over Nakagami-m fading channels, which caters specifically to cell-edge users who rely on line-of-sight (LoS) communication lines from the base station. In [11], the study further explained the closed-form expressions of ergodic rates, revealing insight on the high signal-to-noise ratio (SNR) slopes characteristic of NOMA users, therefore improving the clarity of the system's performance parameters. Moreover, rate-splitting multiple access (RSMA) is a key enabler for efficient radio access in future wireless networks because it outperforms traditional multiple access schemes in terms of spectral efficiency and valuable resource sharing [12], [13]. RSMA divides each users data into separate sub-messages and enables several users to access the same orthogonal resource block [14], [15]. The STAR-IRS Aided NOMA for Short-Packet communications is analysed in terms of block error rate with statistical channel state information (CSI) in [16]. Study [17], shows that NOMA with STAR-IRS enhanced performance than alone IRS, which discusses the average attainable rates of STAR-IRS assisted NOMA employing ES protocol were examined considering the channel correlation. Moreover in [18], the STAR-IRS assisted downlink multiple-input single output (MISO) system is explored

The associate editor coordinating the review of this manuscript and approving it for publication was Oscar Mauricio Caicedo (*Corresponding author: Aswini Krishnan*).

A. Krishnan and S. Maruthu are with the National Institute of Technology, Puducherry, Karaikal, India (e-mails: kaswinikrish@gmail.com, and surendar.m@nitpy.ac.in).

S. Sabapathy is with Amrita Vishwa Vidyapeetham Coimbatore, Coimbatore, India (e-mail: sundaresanece91@gmail.com).

for power utilization minimization. The system is analysed under three protocols viz., time switching, mode switching, and energy splitting for unicast and multicast transmission. The power minimization is achieved through joint optimization of passive transmission, reflection beamforming at the BS and STAR-IRS with data rate constraints. In the literature, most of the works reported on RSMA assisted STAR-IRS considers only the perfect channel conditions. Also, the performance is analysed only in terms of sum rate and outage probability with Rayleigh and Rician fading distributions. To the best of author's knowledge, this is the first work which concentrates on RSMA assisted STAR-IRS system in the presence of channel estimation error and optimal power allocation with weighted sum rate (WSR) maximization technique [19], [20]. The key contributions of this work are:

- We derive the closed form outage probability (OP) of the STAR-IRS assisted RSMA system for perfect and imperfect CSI channel conditions for the transmission (T) and reflection (R) users.
- We perform sum rate analysis and maximize the WSR through automatic optimization (AO) algorithm.
- Also, we optimize the power allocation to achieve minimum outage and maximum sum rate through max-min algorithm for the imperfect channel condition.
- Moreover, we perform Monte-Carlo (MC) simulation for validating the derived numerical analysis on OP and sum rate for the T and R users.
- Finally, we extent the analysis to RSMA assisted IRS and compare the simulation results with RSMA-STAR-IRS system. From the analysis, we show that RSMA assisted STAR-IRS offers enhanced performance than RSMA-IRS system in terms of outage probability.

The rest of the paper is organized as follows. Section II describes the downlink system model of the RSMA-aided STAR-IRS. The system OP, sum rate WSR optimization and power optimization techniques are derived in section III. Whereas, section IV presents the simulation results and its key inferences followed by conclusions in section V.

II. System and Channel Model

The RSMA system with the BS communicating to K users in T and R space through STAR-IRS and no direct transmission, is sketched in Fig. 1. It is assumed that both the users and the BS employ a single antenna. The STAR-IRS serves two type of users viz., the transmitting user U_k^t and reflecting user U_k^r simultaneously, where $k \in \{1, 2, ..., K\}$. The transmitting and reflected users are located behind and front of the STAR-IRS respectively. The IRS surface is assumed to be a uniform planar array (UPA) with $N_k = N_{kh} \times N_{kv}$ elements, where N_{kh} and N_{kv} are the number of elements in the horizontal and vertical directions, respectively. The BS splits the T and R user's information into common part (CP) and private part (PP) through rate splitting and combines all the CPs into a single common stream [21]. Subsequently, the common stream and PP from each user are precoded into common data (CD) and private data (PD). Thus, the superimposed signal contains CD (x_c) and PD $\left(x_k^l\right)$ which is

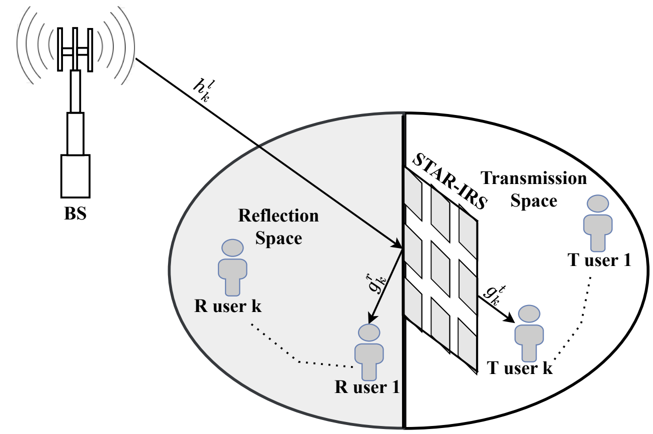

Fig. 1. STAR-IRS aided RSMA communication system with K users.

transmitted over a gamma distribution wireless channel [20] and [22]. Where, l represents both transmitting and reflecting users, $l \in \{t, r\}$. The power allocation for the common and private users are represented as α_c and α_k^l with the condition $\alpha_c + \sum_{k=1}^{K} (\alpha_k^t + \alpha_k^r) = 1$. Hence, the transmitted signal from the BS can be mathematically written as,

$$S = \sqrt{\alpha_c P} x_c + \sum_{k=1}^{K} \left(\sqrt{\alpha_k^t P} x_k^t + \sqrt{\alpha_k^r P} x_k^r \right), \quad (1)$$

where, P is the transmit power used from BS.

A. STAR-IRS Operating Configurations

The STAR RIS's elements can completely transmit, reflect entirely, or both simultaneously, leading to different modes of operation [23]. There are two transmission modes to consider: energy splitting (ES) and mode switching (MS) [23].

1) ES Mode: For RIS elements operating in the ES mode, the transmission and reflection coefficients satisfy $\eta_k^t = \eta_k^r = 1$. RIS elements can transmit and reflect signals simultaneously when they meet the reflection coefficient criteria. Adjusting the SINR expressions for both users served by the same RIS is necessary based on this energy-splitting connection.

2) MS Mode: A signal is reflected to U_k^r by N_k^r elements in MS mode, and transmitted to U_k^t by U_k^t elements, where $N_k = N_k^t + N_k^r$. If $\eta_k^t = 1$ and $\eta_k^r = 0$ are the transmitting elements, and $\eta_k^t = 0$ and $\eta_k^r = 1$ are the reflecting elements. In order to effectively serve both users, MS mode is more constrained than ES mode, allowing just transmission or reflection per element. The SINR calculations are modified based on the reflection coefficients.

The surface components resemble patch antennas made of microstrip. By altering the resonance frequency of every antenna element, with an array spacing of $\frac{\lambda}{2}$, the phase shift is modified to direct the reflected electromagnetic wave in the desired direction. The dimensions of the STAR-IRS surface considered for the analysis is 6×6, and the active elements in the surface are considered as 30. The phase shift is calculated for transmission and reflection using

$\phi_k^t = diag\left(\left[\sqrt{\eta_1^t}e^{j\theta_1^t}, \sqrt{\eta_2^t}e^{j\theta_2^t}, ..\sqrt{\eta_k^t}e^{j\theta_k^t}\right]^T\right)$ and $\phi_k^r = diag\left(\left[\sqrt{\eta_1^r}e^{j\theta_1^r}, \sqrt{\eta_2^r}e^{j\theta_2^r}, ..\sqrt{\eta_k^r}e^{j\theta_k^r}\right]^T\right)$.

B. SINR Characteristics with Perfect CSI (Case-I)

This section analyzes the sum rate, outage probability, and optimal power allocation for RSMA-assisted STAR-IRS under perfect CSI, assuming zero channel estimation error (CEE). The received signal at the k^{th} user is mathematically expressed as,

$$y_k^l = \left((g_k^l)^H \varphi_k^l h_k\right) S + w_k^l, \tag{2}$$

where, w_k^l represents the independent and identically distributed (i.i.d) noise with zero mean and σ^2 variance. The information is transmitted from BS to STAR-IRS via h_k channel and the received information is re-transmitted from the STAR-IRS to the users through $(g_k^l)^H$ channel with phase shift factor φ_k^l. Thus, the CP signal-to-interference plus noise ratio (SINR) for T and R users in RSMA based STAR-IRS system can be expressed as,

$$\gamma_{kc}^l = \frac{\alpha_c P \left|(g_k^l)^H \varphi_k^l h_k\right|^2}{P\sum_{i=1}^K (\alpha_i^t + \alpha_i^r)\left|(g_k^l)^H \varphi_k^l h_k\right|^2 + (\sigma_k^l)^2}. \tag{3}$$

Similarly, the PP SINR can be expressed as,

$$\gamma_{kp}^l = \frac{\alpha_c^l P \left|(g_k^l)^H \varphi_k^l h_k\right|^2}{P\left(\sum_{i=1, i\neq k}^K \alpha_i^l + \sum_{i=1}^K \alpha_i^{\bar{l}}\left|(g_k^l)^H \varphi_k^l h_k\right|^2 + (\sigma_k^l)^2\right)}, \tag{4}$$

Here, $\bar{l} = t$ if $l = r$ and $\bar{l} = r$ if $l = t$.

C. SINR Characteristics with Imperfect CSI (Case-II)

The ideal channel condition is not suitable for practical scenarios due to dynamic nature and multipath effects of the channel. This leads to imperfect channel estimation which is essential to address the inherent challenges posed by dynamic channels, interference, and resource constraints. By accounting for estimation errors, wireless systems can achieve robust and efficient communication in real-world environments. The computed channel between BS to STAR-IRS and STAR-IRS to user is estimated as $\hat{h}_k^l$ and $(\hat{g}_k^l)$. Thus, the received signal at the T and R users in the presence of CEE can be expressed as,

$$\bar{y}_k^l = \left(\left(\hat{g}_k^l + g_{k\varepsilon}^l\right)^H \varphi_k^l \left(\hat{h}_k^l + h_{k\varepsilon}^l\right)\right) S + w_k^l, \tag{5}$$

where, $w_k^l \sim N\left(0, \left(\sigma_k^l\right)^2\right)$ is the i.i.d noise, $g_k^l = \hat{g}_k^l + g_{k\varepsilon}^l$ and $h_k^l = \hat{h}_k^l + h_{k\varepsilon}^l$ such that $\hat{h}_k^l$ and $\hat{g}_k^l$ are the estimated channel coefficients for h_k^l and g_k^l respectively, and $h_{k\varepsilon}^l$ and $g_{k\varepsilon}^l$ are the estimation errors.

After simplification (5) can be rewritten as,

$$\bar{y}_k^l = \left(\left(\hat{g}_k^l\right)^H \varphi_k^l\ \hat{h}_k^l\right) S + w_{k\varepsilon}^l + w_k^l, \tag{6}$$

$w_{k\varepsilon}^l = \left(\left(\hat{g}_k^l\right)^H \varphi_k^l h_{k\varepsilon}^l + \left(g_{k\varepsilon}^l\right)^H \varphi_k^l \hat{h}_k^l + \left(g_{k\varepsilon}^l\right)^H \varphi_k^l h_{k\varepsilon}^l\right) S$ is the term corresponding to error due to imperfect CSI. Using central limit theorem (CLT), the term $w_{k\varepsilon}^l$ can be approximated as Gaussian distributed random variables with variance $\left(\hat{\sigma}^2\right)_{k\varepsilon}^l$. The common message is first decoded at the user's end, and then the appropriate private message is decoded once the common message information has been removed. As a result, while decoding a common message, the private messages behave as an interference term. However, when decoding a private message, all other users' private messages act as an interference term. Utilizing equation (1) in (6), the SINR for the CP and PP at the k^{th} l-type user can be mathematically expressed as [20],

$$\hat{\gamma}_{kc}^l = \frac{\alpha_c P \left|\left(\hat{g}_k^l\right)^H \varphi_k^l \hat{h}_k\right|^2}{P\sum_{i=1}^K \left(\alpha_i^t + \alpha_i^r\right)\left|\left(\hat{g}_k^l\right)^H \varphi_k^l \hat{h}_k\right|^2 + \left(\hat{\sigma}_k^l\right)^2}, \tag{7}$$

$$\hat{\gamma}_{kp}^l = \frac{\alpha_k^l P \left|\left(\hat{g}_k^l\right)^H \varphi_k^l \hat{h}_k\right|^2}{P\left(\sum_{i=1, i\neq k}^K \alpha_i^l + \sum_{i=1}^K \alpha_i^{\bar{l}}\right)\left|\left(\hat{g}_k^l\right)^H \varphi_k^l \hat{h}_k\right|^2 + \left(\hat{\sigma}_k^l\right)^2}, \tag{8}$$

where, $\left(\hat{\sigma}_k^l\right)^2 = \left(\alpha_{k\varepsilon}^l\right)^2 + \left(\alpha_k^l\right)^2$. Let $\left|\hat{g}_k^l \varphi_k^l \hat{h}_k\right|^2 = \left|\sum_{i=1}^K \sqrt{\eta_{ki}^l}\left|\hat{h}_{ki}\right|\left|\hat{g}_{ki}^l\right| e^{j\Delta\varphi ki}\right|^2 = X_k^l$. The reflection coefficient matrix is considered for reflection and transmission side is $\phi_k^t = diag\left(\left[\sqrt{\eta_1^t}e^{j\theta_1^t}, \sqrt{\eta_2^t}e^{j\theta_2^t}, ..\sqrt{\eta_k^t}e^{j\theta_k^t}\right]^T\right)$ and $\phi_k^r = diag\left(\left[\sqrt{\eta_1^r}e^{j\theta_1^r}, \sqrt{\eta_2^r}e^{j\theta_2^r}, ..\sqrt{\eta_k^r}e^{j\theta_k^r}\right]^T\right)$. Where $\Delta\phi_{k_i} = \angle h_{k_i} + \angle g_{k_i}^l + \theta_{k_i}^l$. For optimal transmission, $\Delta\phi_{k_i} = 0$, which can be achieved by setting $\theta_{k_i} = -\left(\angle\hat{h}_{k_i} + \angle\hat{g}_{k_i}^l\right)$. Hence the simplified form of (7) and (8) can be written as,

$$\hat{\gamma}_{kc}^l = \frac{\alpha_c P X_k^l}{P\sum_{k=1}^K \left(\alpha_i^t + \alpha_i^r\right) X_k^l + \left(\hat{\sigma}_k^l\right)^2}. \tag{9}$$

$$\hat{\gamma}_{kp}^l = \frac{\alpha_k^l P X_k^l}{P\left(\sum_{i=1, j\neq k}^K \alpha_i^l \sum_{i=1}^K \alpha_i^l\right) X_k^l + \left(\hat{\sigma}_k^l\right)^2}. \tag{10}$$

D. Channel Distribution Analysis

In this work, the Gamma distribution which plays a crucial role in wireless communication by providing a statistical framework for modeling fading and shadowing effects, facilitating performance analysis, and enabling accurate simulation of wireless channel behavior is exploited. Its importance lies in its ability to capture the stochastic nature of wireless channels, which is essential for designing robust and efficient communication systems. A gamma distribution-based moment-matching technique is used to control the channel distributions of H^l, $l \in \{t, r\}$. The following proposition is provided on the expectation and variance of H^l. Based on the Gamma distribution the expectation and variance of H^l can be written as [21], [22],

$$E\left[H^l\right] = \frac{\pi}{4} N_k, \tag{11}$$

$$Var\left[H^l\right] = \sum_{i=1}^{N_k}\sum_{j=1}^{N_k}\left(\left[\bar{R}_k\right]_{i,j}\right)^2 - \frac{\pi^2}{16} N_K^2, \tag{12}$$

where, $\bar{R}_k \triangleq E\left[|h_k|\,|h_k|^T\right] = E\left[g_k^l\,|g_k|^T\right]$.

For $i \neq j$,

$$\left[\bar{R_k}\right]_{i,j} = \frac{\left|\left[\bar{R_k}\right]_{i,j}\right|^2 - 1}{2} K\left(\left|\left[\bar{R_k}\right]_{i,j}\right|^2\right) + E\left(\left|\left[\bar{R_k}\right]_{i,j}\right|^2\right) \quad (13)$$

For $i = j$,

$$\left[\bar{R_k}\right]_{i,j} = 1 \quad (14)$$

The moment-matching approach can be utilized to analyze the distribution of H_χ by matching the expectation and variance of H_χ to a gamma random variable with mean $k_\chi w_\chi$ and variance $k_\chi w_\chi^2$. As introduced in [22], the gamma distribution can be used to approximate complicated SNR distributions with high accuracy and tractable parameters computations. Thus, H_χ can be approximated as a gamma random variable with shape parameter k_χ and scale parameter w_χ : $k_\chi = \frac{E^2[H_\chi]}{Var[H_\chi]}$ and $w_\chi = \frac{Var[H_\chi]}{E[H_\chi]}$. The probability density function (PDF) and cumulative density function (CDF) of H^l can written as,

$$f_{H_k}(\gamma) \approx \frac{\gamma^{k_\chi} - exp\left(-\frac{\gamma}{w_k}\right)}{\Gamma(k_\chi)\, w_\chi^{k_\chi}}, \quad (15)$$

$$F_{H_k}(\gamma) \approx \frac{1}{\Gamma(k_\chi)} \gamma\left(k_\chi, \frac{\theta}{w_k}\right), \quad (16)$$

where, $f_{H_k}(\gamma)$ represents the PDF of the considered distribution, $F_{H_k}(\gamma)$ indicates the CDF equation.

III. Performance Analysis of RSMA Assisted STAR-IRS System

In this section, the closed form expression for OP and sum rate of RSMA assisted STAR-IRS are derived with the presence of CEE. Also, optimization techniques are adopted for maximizing the WSR and the optimal power allocation ratio is analyzed.

A. Outage Probability

The user experiences an outage if the CP or PP decoding is unsuccessful for the set threshold data rate. The OP of the k^{th} user in terms of CP and PP can be written as,

$$P_{out}^{kl} = (\gamma_{tc}, \gamma_{tp}) = 1 - Pr\left(\gamma_{kc}^l > \gamma_{tc}, \gamma_{kp}^l > \gamma_{tp}\right), \quad (17)$$

where, γ_{tc} and γ_{tp} are the threshold rate for CP and PP respectively. Substituting equation (3) and (4) into (17), the OP of both T and R space users is expressed as,

$$P_{out}^{kl} = \left(\frac{\alpha_c P_{x_k}^l}{P} \sum_{i=1}^{K} \left(\alpha_i^t + \alpha_i^r\right) x_k^l + \hat{\sigma}_k^{l^2}\right). \quad (18)$$

The CP power is always higher than PP, hence outage of CP forces PP also to be in outage. After further simplification, (18) can be rewritten as,

$$P_{out}^{kl} = \left(Xk^l \leq \frac{\gamma_{tc}}{A_c^{kl} - \gamma_{tc} B_c^{kl}}\right), \quad (19)$$

where, $A_c^{kl} = \frac{\alpha_c P}{\hat{\sigma}_k^{l^2}}$, and $B_c^{kl} = \frac{P}{\hat{\sigma} k^{l^2} \sum_{i=1}^{K}\left(\alpha_i^t + \alpha_i^r\right)}$.
Similarly, for the PP message the outage can be written as,

$$P_{out}^{kl} = \left(\frac{\gamma_{tp}}{A_p^{kl} - \gamma_{tp} B_p^{kl}}\right), \quad (20)$$

where, $A_p^{kl} = \frac{\alpha_{kp}^l}{\hat{\sigma}_k^{l^2}}$, and $B_p^{kl} = \frac{P}{\hat{\sigma}_k^{l^2}}$.

B. Sum Rate

The total sum rate for the T and R user's over the Gamma distribution under both perfect and imperfect CSI scenario can be mathematically expressed as [24],

$$R_{PCSI} = log_2\left(1 + \left(\gamma_{kc}^l + \gamma_{kp}^l\right)\right). \quad (21)$$

$$R_{ICSI} = log_2\left(1 + \left(\hat{\gamma}_{kc}^l + \hat{\gamma}_{kp}^l\right)\right). \quad (22)$$

where, R_{PCSI} and R_{ICSI} represents the rate of the user with perfect and imperfect CSI channel condition.

C. WSR Maximization

This paper's prime importance is maximizing the WSR by jointly designing the number of elements in IRS, and its phase shift is the coupled co-efficient constraint. Hence, the optimization problem for maximizing the WSR can be written as [26],

$$E1: \max_{z_k^l \varphi_k^l} f_1\left(z_k^l, \varphi_k^l\right) = \sum_l \sum_{k=1}^{k^l} z_k^l log_2\left(1 + \gamma_k^l\right). \quad (23)$$

s.t

$$\sum_l \sum_{k=l}^{k^l} \left\|z_k^l\right\|^2 \leq P, \quad (24)$$

$$N_{kh} + N_{kv} = 1. \quad (25)$$

$$|\varphi_{kh} - \varphi_{kv}| = \frac{\pi}{2} \; or \; \frac{3\pi}{2}, \quad (26)$$

where, $\varphi_k^l \in [0, 2\pi]$ denotes the phase shift and $N_k \in [0, 1]$ represents the IRS elements.

1) Lagrangian Dual Transformation: According to [[19], [20]], the above mentioned problem can be equivalently written as,

$$\hat{E}_1: \max_{z_k^l \varphi_k^l \alpha_k^l} f_1 \alpha\left(z_k^l \varphi_k^l \alpha_k^l\right) \quad (27)$$

where, α_k^l is an auxiliary variable w.r.t. γ_k^l and $f_1\alpha$ is given in (28), With the conclusion in [23], [25], it is known that for $\hat{E}_1$, when $\left\{z_k^l, \varphi_k^l\right\}$ hold fixed, $\left(\alpha_k^l\right) = \gamma_k^l$. Besides, for a fixed α_k^l, optimizing $\left\{z_k^l, \varphi_k^l\right\}$ is reduced to

$$\hat{E}_1: \max_{z_k^l \varphi_k^l} \sum_l \sum_{k=1}^{k^l} \frac{\gamma_k^l \alpha_k^l}{1 + \gamma_k^l} \quad (29)$$

Now substituting, the SINR values of T and R users to get the WSR using Algorithm 1.

$$f_1\alpha\left(z_k^l\varphi_k^l\alpha_k^l\right) = \sum_l \sum_{k=1}^{k^l} z_k^l log_2\left(1+\alpha_k^l\right) - \sum_l \sum_{k=1}^{k^l} z_k^l \alpha_k^l + \sum_l \sum_{k^l} \frac{z_k^l\left(1+\alpha_k^l\right)\gamma_k^l}{1+\gamma_k^l} \tag{28}$$

Algorithm 1:AO Algorithm

1:Input: Set the initial $\left\{z_k^l, \varphi_k^l\right\}$ and $q=1$

2:Repeat:

a) Update z_k^l by the bisection method

b) Update φ_{kh} and φ_{kv} by the elementwise method

c) $q \leftarrow q+1$

3:Until: $R\left(\left(z_k^l\right)^{q+1}, \left(\varphi_k^l\right)^{q+1}\right) - R\left(\left(z_k^l\right)^q, \left(\varphi_k^l\right)^q\right)$

4:Output: $\left\{z_k^l, \varphi_k^l\right\}$

D. Optimal Power Allocation (Max-Min Power Allocation)

Optimal power allocation is a challenging task in the presence of channel imperfection due to high fading and shadowing. Therefore, the Max-Min method is aided to distribute the optimum power to the user in order to retain performance while tolerating the channel imperfection. The max-min rate problem can be expressed mathematically as estimating a power allocation vector P, which can be solved by,

The method converges when the change in power allocation or objective function is less than the specified threshold. Convergence is ensured if the goal function is convex; otherwise, the method may reach a local optimum. The AO method is very beneficial in power allocation problems because of its simplicity and efficacy in dealing with high-dimensional optimization problems that are challenging to solve directly.

The max-min downlink power update technique in power allocation aims to optimize SINR across all users in a wireless communication network. This strategy assures a fair allocation of power across users, giving the weakest user the highest possible SINR. The system iteratively modifies the power levels assigned to each user, usually beginning with an initial viable power allocation. During each cycle, it adjusts each user's power by solving an optimization problem that optimizes the minimal SINR while considering other users' interference and overall power restrictions. This procedure continues until the SINR values stabilize, guaranteeing that the system's weakest link is optimized, improving overall system performance and fairness. Algorithm 2 can be utilized to achieve optimal power allocation.

Algorithm 2:Max-min downlink power update algorithm

1:Initialize: $P = [P_1, P_2, ..., P_i]$

2:Repeat:

a) Calculate the rate for user:$R_i\left(P\right) = log_2\left(1+\frac{h_iP_i}{\sigma^2+\sum_{i\neq k} h_iP_i}\right)$

b) Update φ_{kh} and φ_{kv} by the elementwise method.

c) $q \leftarrow q+1$

3:Until: $R\left(\left(z_k^l\right)^{q+1}, \left(\varphi_k^l\right)^{q+1}\right) - R\left(\left(z_k^l\right)^q, \left(\varphi_k^l\right)^q\right)$

4:Output: $\left\{z_k^l, \varphi_k^l\right\}$

IV. Results

This section provides numerical and simulation results to validate theoretical analysis. The results show the performance of the R user as a solid line, the performance of the T user as a dashed line, and the analytical results. Also, the markers like ∘, □, ⋄, +, △ and ∗ are used to show the monte carlo simulation results. The key parameters such as power allocation, CEE, perfect CSI are accounted for analysis of T and R users. Fig. 2 shows that the comparison analysis between conventional IRS and STAR-IRS. The different power values such as (0.6, 0.4) and (0.8, 0.2) considered for the users analysis for two different users with (6 × 6) diemension IRS. Generally, the conventional IRS only serves the reflected user and it will not serve the user behind the surface. Hence, Fig. 2 shows the comparison results of conventional IRS and STAR-IRS for R user. Inference reveals that, the T users outage is higher than R users for specific power allocation. This is because the transmission of the signal may cause some loss in the quality of the received signal. Further, the STAR-IRS performance is compared with the conventional IRS model and found the former outperforms the latter. The key factor is that it can transmit and reflect signals simultaneously, increasing signal coverage and intensity on both sides of the surface and improving system performance and spectrum efficiency.

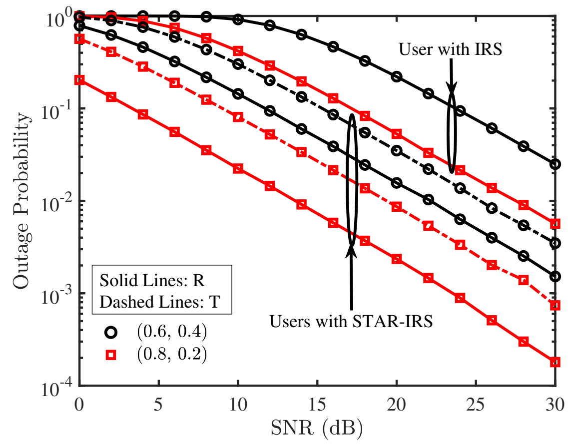

Fig. 2. Comparative analysis of conventional IRS and STAR-IRS based RSMA system.

Fig. 3 depicts the outage probability at various power levels. For the outage analysis threshold value is fixed as 0.5. From the figure it is clearly noted the users achieved less outage at power 0.8 compared to other power levels. Hence, for the considered system 0.8 power level provides the tolerable outage to the users. R user provides better results than the T user because of its reflection process.

Fig. 4 illustrates the sum rate analysis of the system without considering perfect and imperfect CSI scenarios. In this work, two different users are considered for the analysis. Hence, R users achieves sum rate 13 bps and T users achieves 11.2 bps when the power allocation is (0.8, 0.2). For further observation, the power is changed to (0.6, 0.4) then R users achieves 8.3 bps and T users achieves 5 bps. From the figure, it is clearly

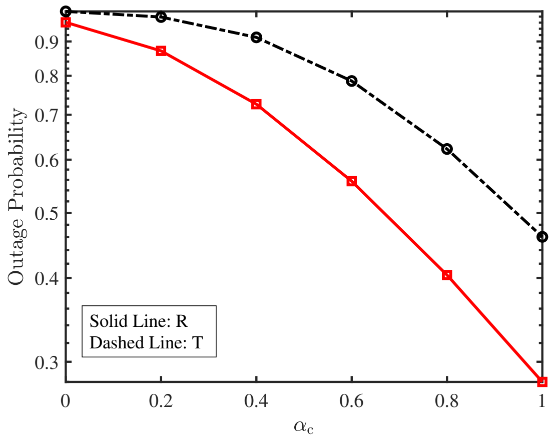

Fig. 3. Outage probability for R and T users based on power levels.

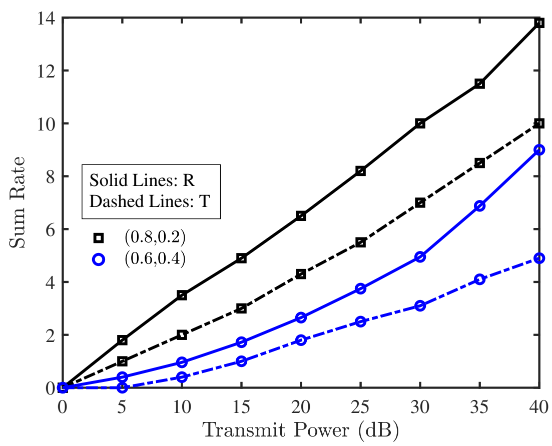

Fig. 4. Sum rate analysis of STAR-IRS based RSMA system for different common and private part power allocation factors.

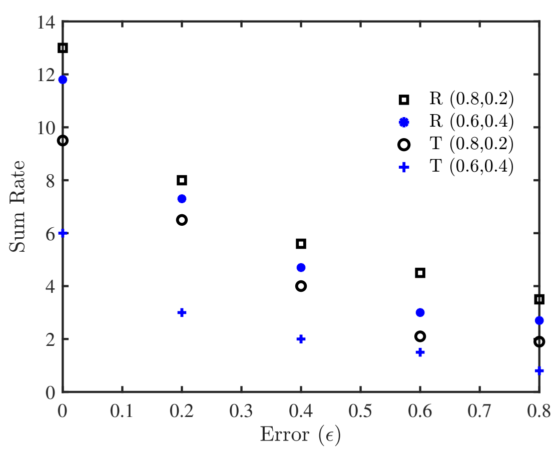

Fig. 5. Sum rate analysis with respect to imperfect CSI error and its analysis for various power allocation factor.

understood that if the power allocation changes, the sum rate also changes.

Fig. 5 demonstrates the users' performance with and without error in the channel during transmission. In the absence of CEE, the system achieves a higher sum rate. The sum rate will degrade because of the error in the system. With the condition mentioned above, the system sum rate is calculated with and without error for T and R users with two different power levels (0.8, 0.2) and (0.6, 0.4).

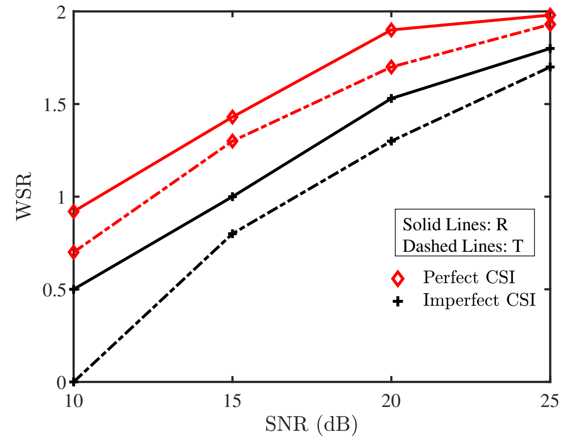

Fig. 6. WSR analysis of STAR-IRS based RSMA system over perfect and imperfect CSI scenarios.

Fig. 6 compares the WSR with SNR values, while the number of elements in the IRS surface is fixed. Here the WSR is increases with SNR values. With perfect scenario the system achieves better WRS value compared to imperfect scenario. The sum capacity decreases during transmission in the system due to the error.

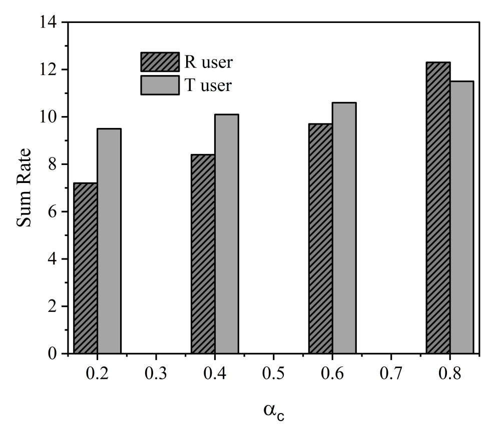

Fig. 7. Common part power optimization through sum rate analysis for STAR-IRS based RSMA system.

The total power allocation of each user's communications makes the above mentioned issues tolerable. As a result, selecting the best power for users will give maximum capacity with transmission error.

Therefore, Fig. 7 depicts the total capacity at various power levels. According to the graph, users' messages reached a tolerable sum rate at power 0.8 compared to other power levels. Over Gamma distribution, the results of the RSMA demonstrate high sum rate transmission with various cases perfect and imperfect CSI with power allocations.

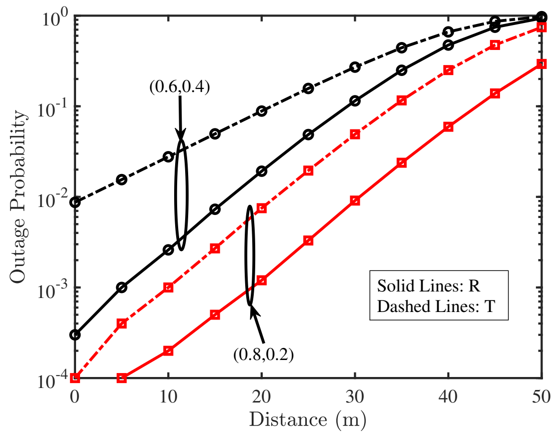

Fig. 8. Outage probability analysis of STAR-IRS based RSMA system with respect to the users distance from the IRS at SNR=50 dB.

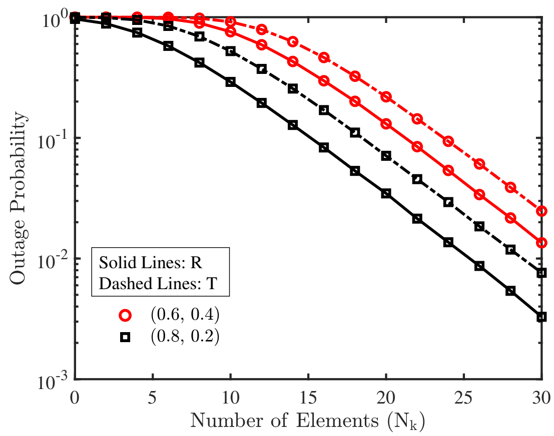

Fig. 9. Outage probability analysis for STAR-IRS based RSMA system with respect to the number of surface elements in STAR-IRS at SNR=50 dB.

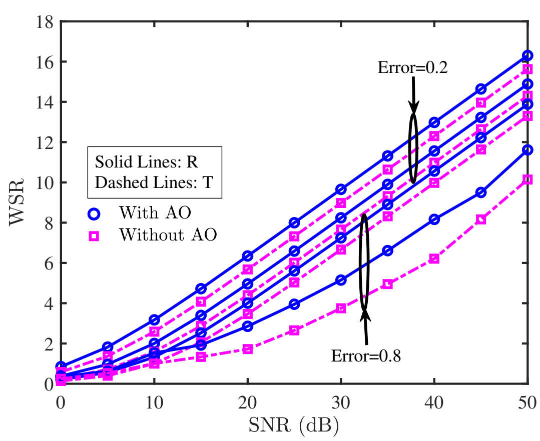

Fig. 10. WSR performance comparison of AO algorithm with conventional algorithm over fixed error values.

The outage probability of a STAR-IRS based RSMA system with respect to the users distance from the STAR-IRS at an SNR of 50 dB is shown in Fig. 8. Strong transmitted and reflected signals are produced when the user is near, which reduces the probability of an outage because of efficient signal enhancement. Even at high SNR, the path loss rises with user distance, leading to worse signal reception. As a result, as the IRS's potential to adapt for signal loss decreases with distance, the probability of an outage increases. The result indicates that the users' distance from the STAR-IRS significantly assesses the system's reliability even under optimal SNR circumstances.

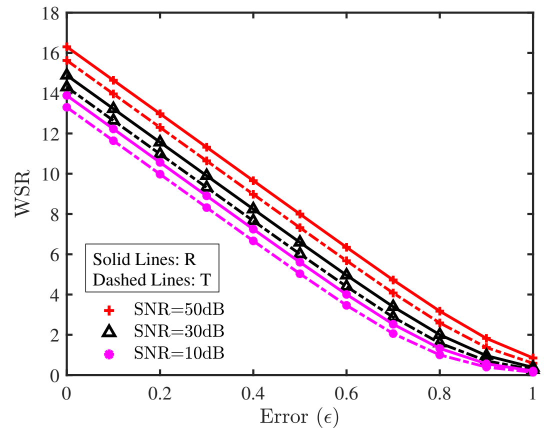

Fig. 11. WSR analysis of AO algorithm employed STAR-IRS based RSMA system over various values of imperfect CSI error.

The outage probability of an RSMA system based on STAR-IRS concerning the surface element count is shown in Fig. 9. As a result, the outage probability decreases as the number of surface elements increases. Fig. 10 illustrates a comparative study of WSR with and without the AO algorithm. The analysis considers fixed error values of $\epsilon = 0.2$ and $\epsilon = 0.8$. With these constant error levels, the performance of WSR is assessed. The results clearly show that the WSR is significantly improved when the AO algorithm is applied compared to when it is not implemented. Fig. 11 illustrates WSR analysis with the effect of varying error ϵ. As the SNR values increase, the performance improves. This trend highlights the positive correlation between higher SNR and enhanced system performance.

V. Conclusion

The study focused on exploring ways to improve the performance of the downlink system, particularly in terms of enhancing each user's weighted sum rate and outage performance of the STAR-IRS system. The closed-form expressions of outage probability is derived to evaluate the system performance. Also, the behavior of the sum rate is analyzed under various conditions, including perfect and imperfect CSI scenarios over the Gamma distribution. Additionally, the optimal power allocation is determined through an automatic optimization algorithm.The statistical data offer insights into the impact of errors on the sum rate. To improve the study, it would be helpful to delve more into the specific approaches or schemes offered to increase performance. Additionally, underlining any practical implications of the results and indicating areas for future research or implementation will improve clarity and efficiency of the system model considered.

References

[1] C. Huang, A. Zappone, G. C. Alexandropoulos, M. Debbah and C. Yuen, "Reconfigurable Intelligent Surfaces for Energy Efficiency in Wireless Communication," in IEEE Transactions on Wireless Communications, vol. 18, no. 8, pp. 4157-4170, Aug. 2019, doi: 10.1109/TWC.2019.2922609.

[2] S. Hu, F. Rusek and O. Edfors, "Beyond Massive MIMO: The Potential of Data Transmission With Large Intelligent Surfaces," in IEEE Transactions on Signal Processing, vol. 66, no. 10, pp. 2746-2758, 15 May15, 2018, doi: 10.1109/TSP.2018.2816577.

[3] M. Cui, G. Zhang and R. Zhang, "Secure Wireless Communication via Intelligent Reflecting Surface," in IEEE Wireless Communications Letters, vol. 8, no. 5, pp. 1410-1414, Oct. 2019, doi: 10.1109/LWC.2019.2919685.

[4] Q. Wu and R. Zhang, "Towards Smart and Reconfigurable Environment: Intelligent Reflecting Surface Aided Wireless Network," in IEEE Communications Magazine, vol. 58, no. 1, pp. 106-112, January 2020, doi: 10.1109/MCOM.001.1900107.

[5] L. Sanguinetti, E. Björnson and J. Hoydis, "Toward Massive MIMO 2.0: Understanding Spatial Correlation, Interference Suppression, and Pilot Contamination," in IEEE Transactions on Communications, vol. 68, no. 1, pp. 232-257, Jan. 2020, doi: 10.1109/TCOMM.2019.2945792.

[6] H. Guo, Y. -C. Liang, J. Chen and E. G. Larsson, "Weighted Sum-Rate Maximization for Intelligent Reflecting Surface Enhanced Wireless Networks," 2019 IEEE Global Communications Conference (GLOBECOM), Waikoloa, HI, USA, 2019, pp. 1-6, doi: 10.1109/GLOBECOM38437.2019.9013288.

[7] Yu, Xianghao, Dongfang Xu, and Robert Schober. "MISO wireless communication systems via intelligent reflecting surfaces." 2019 IEEE/CIC International Conference on Communications in China (ICCC). IEEE, 2019, doi:10.48550/arXiv.1904.12199.

[8] J. Xu, Y. Liu, X. Mu and O. A. Dobre, "STAR-RISs: Simultaneous Transmitting and Reflecting Reconfigurable Intelligent Surfaces," in IEEE Communications Letters, vol. 25, no. 9, pp. 3134-3138, Sept. 2021, doi: 10.1109/LCOMM.2021.3082214.

[9] Xu, Jiaqi, et al. "STAR-RISs: Simultaneous transmitting and reflecting reconfigurable intelligent surfaces." IEEE Communications Letters 25.9 (2021), doi:10.48550/arXiv.2101.09663.

[10] H. Niu, Z. Chu, F. Zhou, P. Xiao and N. Al-Dhahir, "Weighted Sum Rate Optimization for STAR-RIS-Assisted MIMO System," in IEEE Transactions on Vehicular Technology, vol. 71, no. 2, pp. 2122-2127, Feb. 2022, doi: 10.1109/TVT.2021.3131568.

[11] Zhao, Boqun, et al. "Ergodic rate analysis of STAR-RIS aided NOMA systems." IEEE Communications Letters 26.10 (2022), doi:10.48550/arXiv.2207.11304.

[12] O. Dizdar, Y. Mao, W. Han and B. Clerckx, "Rate-Splitting Multiple Access: A New Frontier for the PHY Layer of 6G," 2020 IEEE 92nd Vehicular Technology Conference (VTC2020-Fall), Victoria, BC, Canada, 2020, pp. 1-7, doi: 10.1109/VTC2020-Fall49728.2020.9348672.

[13] Park, Jeonghun, et al. "Rate-splitting multiple access for 6G networks: Ten promising scenarios and applications." IEEE Network (2023), doi:10.48550/arXiv.2306.12978.

[14] Dizdar, Onur, Yijie Mao, and Bruno Clerckx. "Rate-splitting multiple access to mitigate the curse of mobility in (massive) MIMO networks." IEEE Transactions on Communications 69.10 (2021), doi:10.48550/arXiv.2102.06405

[15] Mao, Yijie, Bruno Clerckx, and Victor OK Li. "Rate-splitting multiple access for downlink communication systems: Bridging, generalizing, and outperforming SDMA and NOMA." EURASIP journal on wireless communications and networking 2018 (2018), doi:10.1186/s13638-018-1104-7.

[16] J. Xu, L. Yuan, N. Yang, N. Yang and Y. Guo, "Performance Analysis of STAR-IRS Aided NOMA Short-Packet Communications With Statistical CSI," in IEEE Transactions on Vehicular Technology, vol. 72, no. 9, pp. 12385-12390, Sept. 2023, doi: 10.1109/TVT.2023.3266830.

[17] Y. Mao, B. Clerckx and V. O. K. Li, "Rate-Splitting Multiple Access for Coordinated Multi-Point Joint Transmission," 2019 IEEE International Conference on Communications Workshops (ICC Workshops), Shanghai, China, 2019, pp. 1-6, doi: 10.1109/ICCW.2019.8756668.

[18] H. Dahrouj and W. Yu, "Multicell Interference Mitigation with Joint Beamforming and Common Message Decoding," in IEEE Transactions on Communications, vol. 59, no. 8, pp. 2264-2273, August 2011, doi: 10.1109/TCOMM.2011.060911.100554.

[19] S. Dhok and P. K. Sharma, "Rate-Splitting Multiple Access With STAR RIS Over Spatially-Correlated Channels," in IEEE Transactions on Communications, vol. 70, no. 10, pp. 6410-6424, Oct. 2022, doi: 10.1109/TCOMM.2022.3198121.

[20] Guo, Huayan, et al. "Weighted sum-rate maximization for reconfigurable intelligent surface aided wireless networks." IEEE transactions on wireless communications 19.5 (2020), doi:10.48550/arXiv.1912.11999

[21] S. Atapattu, C. Tellambura and H. Jiang, "A Mixture Gamma Distribution to Model the SNR of Wireless Channels," in IEEE Transactions on Wireless Communications, vol. 10, no. 12, pp. 4193-4203, December 2011, doi: 10.1109/TWC.2011.111210.102115.

[22] S. Al-Ahmadi and H. Yanikomeroglu, "On the approximation of the generalized-κ distribution by a gamma distribution for modeling composite fading channels," in IEEE Transactions on Wireless Communications, vol. 9, no. 2, pp. 706-713, February 2010, doi: 10.1109/TWC.2010.02.081266.

[23] X. Mu, Y. Liu, L. Guo, J. Lin and R. Schober, "Simultaneously Transmitting and Reflecting (STAR) RIS Aided Wireless Communications," in IEEE Transactions on Wireless Communications, vol. 21, no. 5, pp. 3083-3098, May 2022, doi: 10.1109/TWC.2021.3118225.

[24] X. Mu, Y. Liu, L. Guo, J. Lin and R. Schober, "Simultaneously Transmitting and Reflecting (STAR) RIS Aided Wireless Communications," in IEEE Transactions on Wireless Communications, vol. 21, no. 5, pp. 3083-3098, May 2022, doi: 10.1109/TWC.2021.3118225.

[25] Zuo, Jiakuo, et al. "Joint design for simultaneously transmitting and reflecting (STAR) RIS assisted NOMA systems." IEEE Transactions on Wireless Communications 22.1 (2022), doi:10.48550/arXiv.2106.03001.

[26] Niu, Hehao, and Xiaohu Liang. "Weighted sum-rate maximization for STAR-RISs-aided networks with coupled phase-shifters." IEEE Systems Journal 17.1 (2022): 1083-1086, doi:10.1109/JSYST.2022.3159551.

Aswini Krishnan (Graduate Student Member, IEEE) received her Bachelor in Engineering Degree in Electronics and Instrumentation Engineering and the Master of Engineering Degree in VLSI Design from Anna University, Chennai, India, in 2018 and 2020 respectively. Currently she is pursuing her Ph.D. in Wireless Communication in the Department of Electronics and Communication Engineering, National Institute of Technology (NIT), Puducherry, India. She is a recipient of MHRD Scholarship for her Ph.D Program in the Department of Electronics and Communication Engineering, National Institute of Technology (NIT), Puducherry, India. Her research interests include NOMA, RSMA, Wireless Communication, 5G and Beyond Applications.

Sundaresan Sabapathy (Graduate Student Member, IEEE) received his Doctoral degree from National Institute of Technology Puducherry, Karaikal in Wireless Communications, M.Tech degree in Remote Sensing and Wireless Sensor Networks from Amrita Vishwa Vidyapeetham, Coimbatore and B.Tech (ECE) degree from Pondicherry University, Puducherry and. He has 5 years of teaching experience and have published several research articles and book chapters in various reputed journals and international conferences. He is currently working as Assistant Professor in School of AI, Amrita Vishwa Vidyapeetham, Coimbatore. His research interests are Software Defined Radio, URLLC, PHY Layer design, 5G and Beyond systems.

Surendar Maruthu (Member, IEEE) received his Bachelor in Engineering Degree Electronics and Communication Engineering (2010) and Master of Engineering Degree in Wireless Technologies (2012) from Thiagarajar College of Engineering, Madurai, Tamilnadu, India. He obtained his Ph.D. degree in wireless communication from the National Institute of Technology, Tiruchirappalli (NITT), India in 2017. He is currently working as an Assistant Professor in the Department of Electronics and Communication Engineering, National Institute of Technology, Puducherry (NITPY), India. His research interests include massive MIMO, Physical layer, unmanned aerial vehicles and machine learning. He published his research papers in referred international journals and international conferences.